

Self-Assembly of Antimicrobial Peptoids Impacts Their Biological Effects on *ESKAPE* Bacterial Pathogens

Josefine Eilsø Nielsen,[▽] Morgan Ashley Alford,[▽] Deborah Bow Yue Yung,[▽] Natalia Molchanova, John A. Fortkort, Jennifer S. Lin, Gill Diamond, Robert E. W. Hancock, Håvard Jenssen, Daniel Pletzer, Reidar Lund, and Annelise E. Barron*



Cite This: *ACS Infect. Dis.* 2022, 8, 533–545



Read Online

ACCESS |



Metrics & More



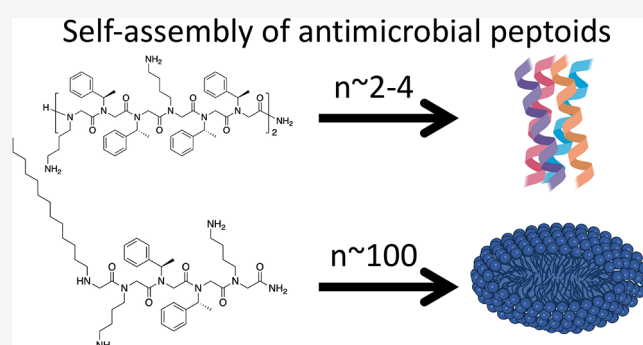
Article Recommendations



Supporting Information

ABSTRACT: Antimicrobial peptides (AMPs) are promising pharmaceutical candidates for the prevention and treatment of infections caused by multidrug-resistant *ESKAPE* pathogens, which are responsible for the majority of hospital-acquired infections. Clinical translation of AMPs has been limited, in part by apparent toxicity on systemic dosing and by instability arising from susceptibility to proteolysis. Peptoids (sequence-specific oligo-*N*-substituted glycines) resist proteolytic digestion and thus are of value as AMP mimics. Only a few natural AMPs such as LL-37 and polymyxin self-assemble in solution; whether antimicrobial peptoids mimic these properties has been unknown. Here, we examine the antibacterial efficacy and dynamic self-assembly in aqueous media of eight peptoid mimics of cationic AMPs designed to self-assemble and two nonassembling controls. These amphipathic peptoids self-assembled in different ways, as determined by small-angle X-ray scattering; some adopt helical bundles, while others form core–shell ellipsoidal or worm-like micelles. Interestingly, many of these peptoid assemblies show promising antibacterial, antibiofilm activity *in vitro* in media, under host-mimicking conditions and antiabscess activity *in vivo*. While self-assembly correlated overall with antibacterial efficacy, this correlation was imperfect. Certain self-assembled morphologies seem better-suited for antibacterial activity. In particular, a peptoid exhibiting a high fraction of long, worm-like micelles showed reduced antibacterial, antibiofilm, and antiabscess activity against *ESKAPE* pathogens compared with peptoids that form ellipsoidal or bundled assemblies. This is the first report of self-assembling peptoid antibacterials with activity against *in vivo* biofilm-like infections relevant to clinical medicine.

KEYWORDS: peptoids, micelles, antibacterial, biofilm, abscess, infection



INTRODUCTION

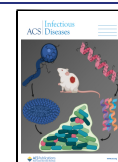
Natural antimicrobial peptides (AMPs) and their synthetic mimics¹ have emerged as promising therapeutics for treating infections caused by multidrug-resistant pathogens due to their broad-spectrum activity against both Gram-negative and Gram-positive bacteria.² AMPs are diverse, short (generally <40 amino acids), amphipathic, positively charged (+2 to +9 net charge) biomolecules found in all forms of life.³ In addition to their own potent antimicrobial activity, AMPs act synergistically in conjunction with traditional antibiotics. This property may reduce the induction of antimicrobial tolerance and resistance.⁴ We have developed peptidomimetics, known as peptoids, which are synthetic oligomers that mimic peptide structures.⁵ Peptoids are based on the same sequence of backbone atoms as natural peptides but are less susceptible to proteolysis and enzymatic degradation because their functional side chains are appended to the backbone nitrogen (N) atom rather than to the α -carbon atom.⁶ Peptoids are therefore sequence-specific *N*-substituted gly-

cines. Peptoid AMP mimics studied to date consisted of a relatively small number of different monomers and typically were less than ~ 13 monomers in length.⁷ *N*-substitution of the peptoid backbone prevents it from serving as a hydrogen-bond donor. Nonetheless, peptoids with certain sequences form stable secondary structures, such as helices.^{8,9}

It has been previously suggested that a relatively high number of peptoid residues is required to achieve sufficient levels of attractive side chain interactions for self-assembly, since backbone–backbone hydrogen bonding is restricted and flexibility is increased in peptoids relative to peptides.¹⁰

Received: October 12, 2021

Published: February 17, 2022



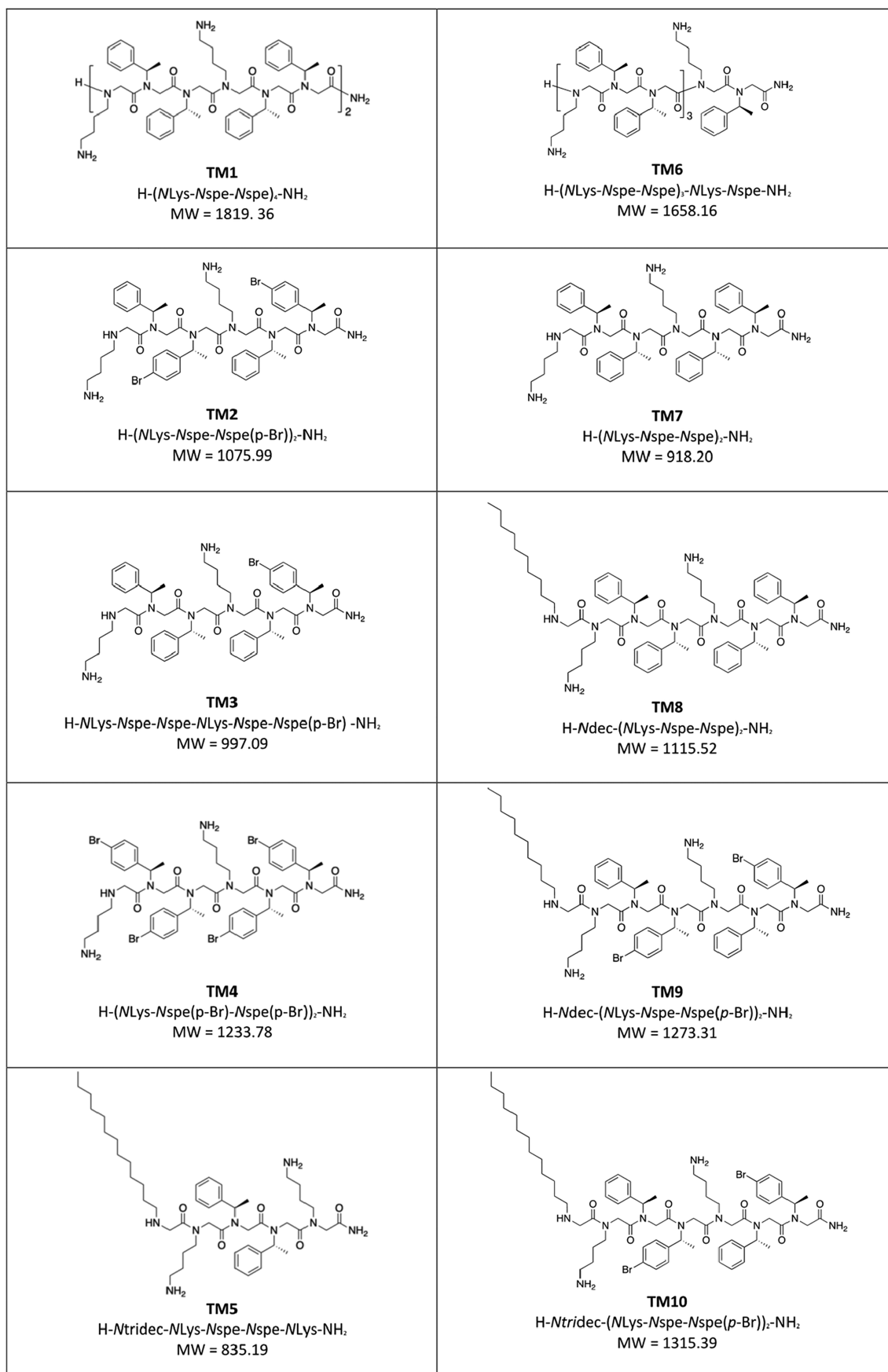


Figure 1. Chemical structures of the peptoids, TM1-10, included in this study, as previously presented in ref 14.

Covalent attachment of lipophilic tail residues can promote self-assembly by enhancing intermolecular hydrophobic interactions, inducing the formation of micellar macromolecular assemblies.^{11,12} Self-assembly of short, water-soluble, linear peptoids has also been demonstrated in the absence of chirality, hydrogen-bonding, and charge group deionization.¹⁰ Therefore, in some instances, increased flexibility of the peptoid backbone can aid self-assembly due to accommodation of π - π stacking and hydrogen bonding between side chains.¹⁰ Furthermore, we previously showed in Molchanova et al. how sequence length, degree of halogen substitution, and halogen identity all impact the self-assembly of peptoids, which in turn affects the antimicrobial activity.¹³ In the present work, we explored the relationship between self-assembly and biological activity against *ESKAPE* pathogens of a series of 10 peptoids¹⁴ (with and without lipid tails or halogen substitution), based on the previously described Peptoid 1⁵ referred to herein as TM1 and another peptoid previously referred to as Peptoid 2 or 1-C13_{4mer}^{15–17} (referred to herein as TMS).

The *ESKAPE* pathogens are six species of bacteria that are the primary cause of nosocomial (hospital-acquired) infections exhibiting virulence and multidrug resistance.¹⁸ These species, including *Enterococcus faecium*, *Staphylococcus aureus*, *Klebsiella pneumoniae*, *Acinetobacter baumannii*, *Pseudomonas aeruginosa*, and *Enterobacter spp.*, have the propensity to form biofilms through a process of surface attachment, production of extracellular matrix, and maturation.¹⁸ Biofilm-forming bacteria often exist in densely populated communities (>10⁷ CFU/mL) and are associated with ~65 and ~80% of all microbial and chronic infections, respectively.¹⁹ Current treatment regimens for biofilm infections are not standardized and typically feature physical or mechanical removal of the biofilm (debridement) followed by antibiotic therapy using broad-spectrum antimicrobials.²⁰ These treatments are often ineffective due to the ability of components of the biofilm to interfere with antibiotic activity²¹ and the slower metabolic activity of organisms encapsulated deep within the biofilm architecture.^{22,23} Thus, there is an urgent need for new therapeutics with low induction of canonical resistance mechanisms in conjunction with potent antibiofilm activity.^{24,25}

We found that while the relationship between self-assembly and biofunctionality of the peptoids was complex, all active antimicrobial peptoids did form stable supramolecular assemblies. Several newly described supramolecular peptoid assemblies exhibited antimicrobial, antibiofilm, and antiabscess activity against selected *ESKAPE* pathogens both in standard laboratory media and under host-mimicking conditions *in vitro* and *in vivo*. This activity persisted, even though small-angle X-ray scattering (SAXS) data showed that the peptoids adopted distinct macromolecular structures. Remarkably, certain peptoids retained their antibiofilm activity in the context of polymicrobial infections comprising clinical isolates of *P. aeruginosa* and *S. aureus* under host-mimicking conditions *in vitro*, while appearing to be safe and nontoxic to human cells even at concentrations as high as 256 $\mu\text{g/mL}$. Therefore, certain self-assembling peptoids described here offer good potential for development as anti-infective agents for the prevention and treatment of nosocomial infections caused by *ESKAPE* pathogens.

RESULTS

Peptoids Self-Assembled into Different Defined Nanostructures. Ten different peptoid AMP mimics, which

were previously reported as antivirals active against Herpes Simplex Virus HSV-1 and SARS-CoV-2,¹⁴ were investigated herein as self-assembling antibacterial AMP mimics. LL-37 is an example of a self-assembling human antibacterial peptide that is also active against SARS-CoV-2.^{26,27} Of these ten peptoids, four were designed with terminal *N*-decyl or *N*-tridecyl alkyl tails, while all peptoids comprised α -chiral, aromatic *N*spe, and cationic lysine-like *N*Lys residues (Figure 1). A detailed discussion of how the studied library of peptoids was designed was described previously.¹⁴ We investigated the self-assembly of these peptoids (except TM3) and of the natural human antimicrobial peptide LL-37 using SAXS (Figure 2). Based on theoretical model analysis (Supporting

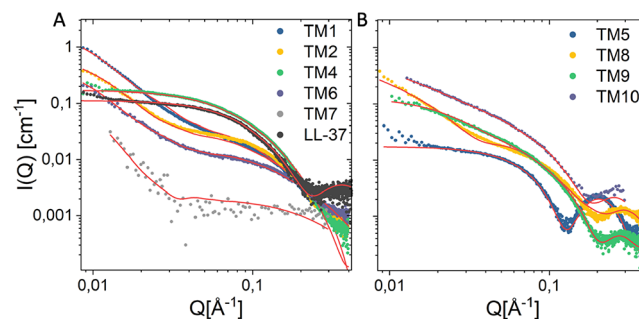


Figure 2. Comparison of SAXS data of peptoids (4 mM) and LL-37 plotted together with best fit (red line) using models described in the Supporting Information. Peptoids could be distinguished according to their class and are presented as groups of peptoids and peptides (A) or lipopeptoids (B).

Information Section 1.2 for details of models), the self-assembled structures of the peptoids in aqueous solution were determined (Figure 3). The peptoids without alkyl chains formed helical bundles either as dimers, trimers, or/and tetramers (Figures 2A and 3A). The 12mer peptoid TM1, whose prior studies have shown to be helical in the secondary structure in association with anionic lipid micelles,^{5,28} assembled mostly into dimers but also demonstrated a smaller fraction of monomers and larger bundles (trimers/tetramers could not be distinguished in this mixture). TM6, an 11-mer version of TM1 lacking one C-terminal *N*spe monomer, formed dimers and monomers with no larger bundles. This suggests that *N*spe monomers are important for the intermolecular assembly of this class of peptoids, as seen in prior studies.²⁹ TM7, a 6-mer version comprising one-half of TM1, was the only peptoid in the series that exhibited Gaussian chain morphology without a higher order structure [with just a 0.003% fraction of larger aggregates (dimensions of 110 Å × 350 Å × > 1000 Å)], consistent with its shorter length. Helicity also might be important for self-assembly of this class of water-soluble peptoids due to their three-faced helical structures, and the known driving forces of assembly of amphipathic helices into bundles or coiled coils to bury the hydrophobic side chains on two faces of the TM1 peptoid helix.³⁰ Helicity was previously found to be dependent on peptoid chain length.⁹

The halogen-substituted peptoids TM2 and TM4 formed larger helical bundles (estimated to be tetramers based on theoretical modeling), likely through an effective “hydrophobic” interaction between the heavy bromine para-benzyl substituent atoms. TM2 (which includes two *N*spe monomers with bromine substitutions) included a 0.005% fraction of

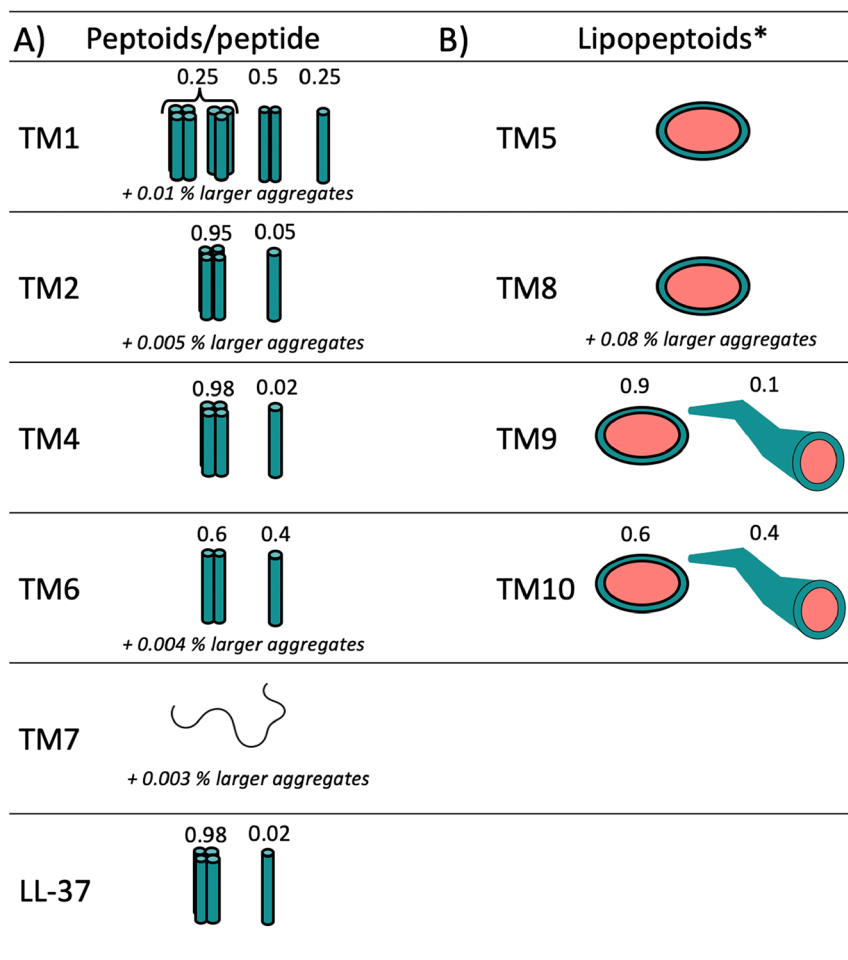


Figure 3. Morphology of peptoid/peptide aggregates based on best fit analysis of SAXS data. (A) Monomers or helical bundles and (B) core–shell ellipsoidal or worm-like micelles. The percentage of larger aggregates refers to the presence of a very small fraction of larger filaments seen from the sharp upturn at low Q in the scattering patterns. *Structure above the CMC, which was undetectably low (in the order of $1 \mu\text{g/mL}$).

Table 1. MIC ($\mu\text{g/mL}$) of Peptoids against ESKAPE Pathogens in MHB Except for *E. faecium* #2–1, which Was Determined in TSB Supplemented with 1% Glucose

	TM1	TM2	TM3	TM4	TM5	TM7	TM8	TM9	TM10
<i>E. faecium</i> #2–1	1.56	1.56	6.25	0.78	1.56	25	0.78	3.13	12.5
<i>S. aureus</i> USA300 LAC	1.56	6.25	50	6.25	1.56	100	3.13	1.56	12.5
<i>K. pneumoniae</i> KPLN649	6.25	12.5	50	12.5	25	>100	12.5	50	>100
<i>A. baumannii</i> ABS075	3.13	25	>100	3.13	12.5	>100	3.13	6.25	100
<i>P. aeruginosa</i> LESB58	12.5	12.5	25	6.25	3.13	50	6.25	12.5	25
<i>E. cloacae</i> 218R1	6.25	100	>100	12.5	25	>100	12.5	12.5	50

larger aggregates (dimensions of $120 \text{ \AA} \times 280 \text{ \AA} \times > 1000 \text{ \AA}$), seen as a sharp upturn at low Q ($\sim 0.009\text{--}0.03$) (Figure 2A), while TM4 did not exhibit any of these larger aggregates. Interestingly, the SAXS pattern of TM4 was very similar to that of the human peptide LL-37 (included for comparison) (Figures 2A and 3A).

The scattered intensity obtained from the alkylated lipopeptoids exhibited a classical core–shell scattering pattern with clear oscillations, thus indicating the presence of micellar structures, which is expected due to the enhanced intermolecular hydrophobic interactions when introducing the alkyl tails.^{11,12} Interestingly, model analysis determined that TM5, a C13-terminated peptoid pentamer, formed ellipsoidal micellar assemblies with $R_{\text{core}} = 13 \text{ \AA}$, an eccentricity (ϵ) of 1.6 and a dR of 7 \AA . Peptoid TM8, a C10-terminated

heptamer, also formed ellipsoidal micellar assemblies but with a slightly smaller $R_{\text{core}} = 10 \text{ \AA}$ reflecting the shorter aliphatic tail, an $\epsilon = 1.9$, and a slightly thicker shell as shown by a $dR = 9 \text{ \AA}$. TM8 exhibited an upturn at low Q indicating the presence of a small ($\sim 0.08\%$) fraction of bigger aggregates (dimensions of $150 \text{ \AA} \times 280 \text{ \AA} \times > 1000 \text{ \AA}$). TM9 and TM10 are brominated versions of TM8 with either *N*-decyl or *N*-tridecyl amino-terminal tails, which assembled into mixtures of ellipsoids and longer worm-like micelles. While TM9 exhibited a relatively small (0.1%) fraction of worm-like micelles, this fraction was significantly higher for TM10 (0.4%).

Self-Assembling Peptoids Inhibit the Growth of ESKAPE Pathogens. We previously showed that at low micromolar concentrations ($12.5 \mu\text{M}$), TM1 inhibited the growth of *P. aeruginosa*¹⁷ and other clinically relevant Gram-

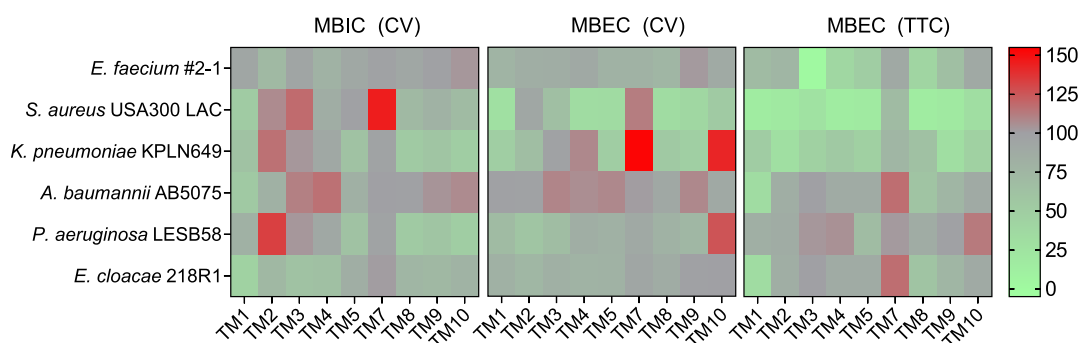


Figure 4. Biofilm inhibition and eradication of *ESKAPE* pathogens at the lowest concentration of peptoid tested. In MBIC assays, 1.56 $\mu\text{g}/\text{mL}$ of peptoid was used. In MBEC assays, 6.25 $\mu\text{g}/\text{mL}$ of peptoid was used to treat *A. baumannii* but 12.5 $\mu\text{g}/\text{mL}$ was used to treat all other species relative to PBS (%). Biofilm inhibition was measured by CV staining, and eradication was measured by CV staining and TTC reduction. Results from three independent experiments ($n = 3$) are displayed as a mean using a gray-scale gradient where green indicates less biofilm (<75%) and red indicates more biofilm (>120%).

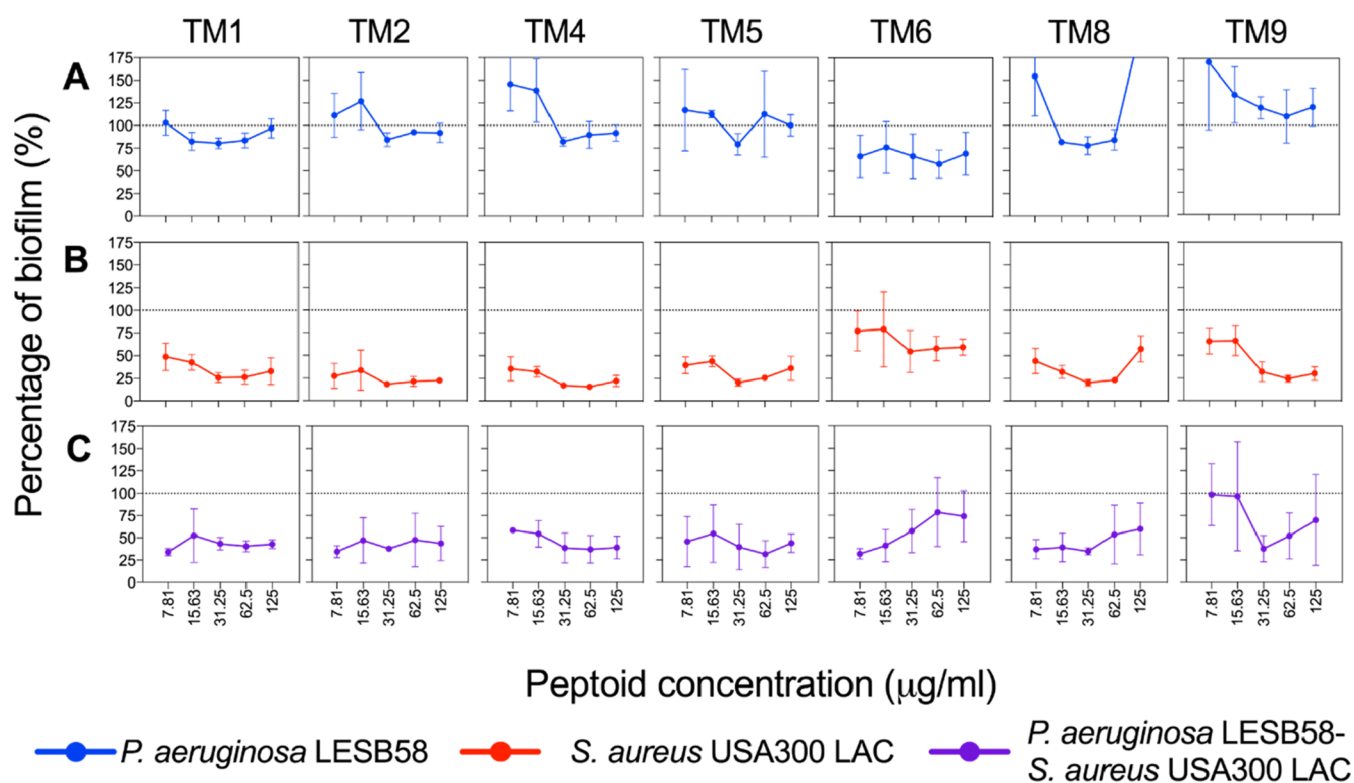


Figure 5. Effect of peptoids under host-mimicking conditions on mono- and polymicrobial biofilm eradication. (A) *P. aeruginosa* LESB58 (5×10^5 CFU/mL) and (B) *S. aureus* USA300 LAC (2.5×10^7 CFU/mL) mono- and (C) polymicrobial biofilms were grown for 20–24 h in DMEM-FBS-G prior to treatment with peptoids. Biofilms were stained with CV (0.1%) after an additional 24 h. Values were normalized to the biofilm growth control, which is indicated by the dotted line. Data from three independent experiments ($n = 3$) are presented as the mean \pm SEM.

negative and Gram-positive pathogens, including *Escherichia coli*, *K. pneumoniae*, *E. faecalis*, and *S. aureus*.³¹ Here, we built on these studies using clinical isolates of the *ESKAPE* pathogens to assess the efficacy of this library of ten different peptoids, which contained eight novel compounds. TM1 inhibited the growth of all *ESKAPE* pathogens at 1.56–12.5 $\mu\text{g}/\text{mL}$ (Table 1). TM2 inhibited *E. faecium* and *P. aeruginosa* at the same concentrations as TM1 (1.56 and 12.5 $\mu\text{g}/\text{mL}$, respectively), but higher concentrations were needed to inhibit the growth of the other bacterial species. Similarly, TM4 inhibited *E. faecium* and *P. aeruginosa* at lower concentrations (0.78 and 6.25 $\mu\text{g}/\text{mL}$, respectively) than TM1, but equal or higher concentrations were needed to inhibit other species.

TM5 inhibited the growth of *E. faecium*, *S. aureus*, and *P. aeruginosa* at concentrations equal to or less than those for TM1, whereas TM8 showed equal or improved activity toward *E. faecium*, *A. baumannii*, and *P. aeruginosa*. In contrast, TM3, TM7, TM9, and TM10 exhibited equal or worse inhibitory activity toward all *ESKAPE* pathogens. This is intriguing since TM9 and TM10 formed worm-like micelles, which seems to be detrimental to the activity of these peptoids against *ESKAPE* pathogens.

No Apparent Cytotoxicity of Peptoids In Vitro Using Primary Human Gingival Cell Cultures. Peptoids TM1, TM2, TM3, TM4, TM5, TM6, and TM9 (which we considered to be of interest as lead antibacterial compounds)

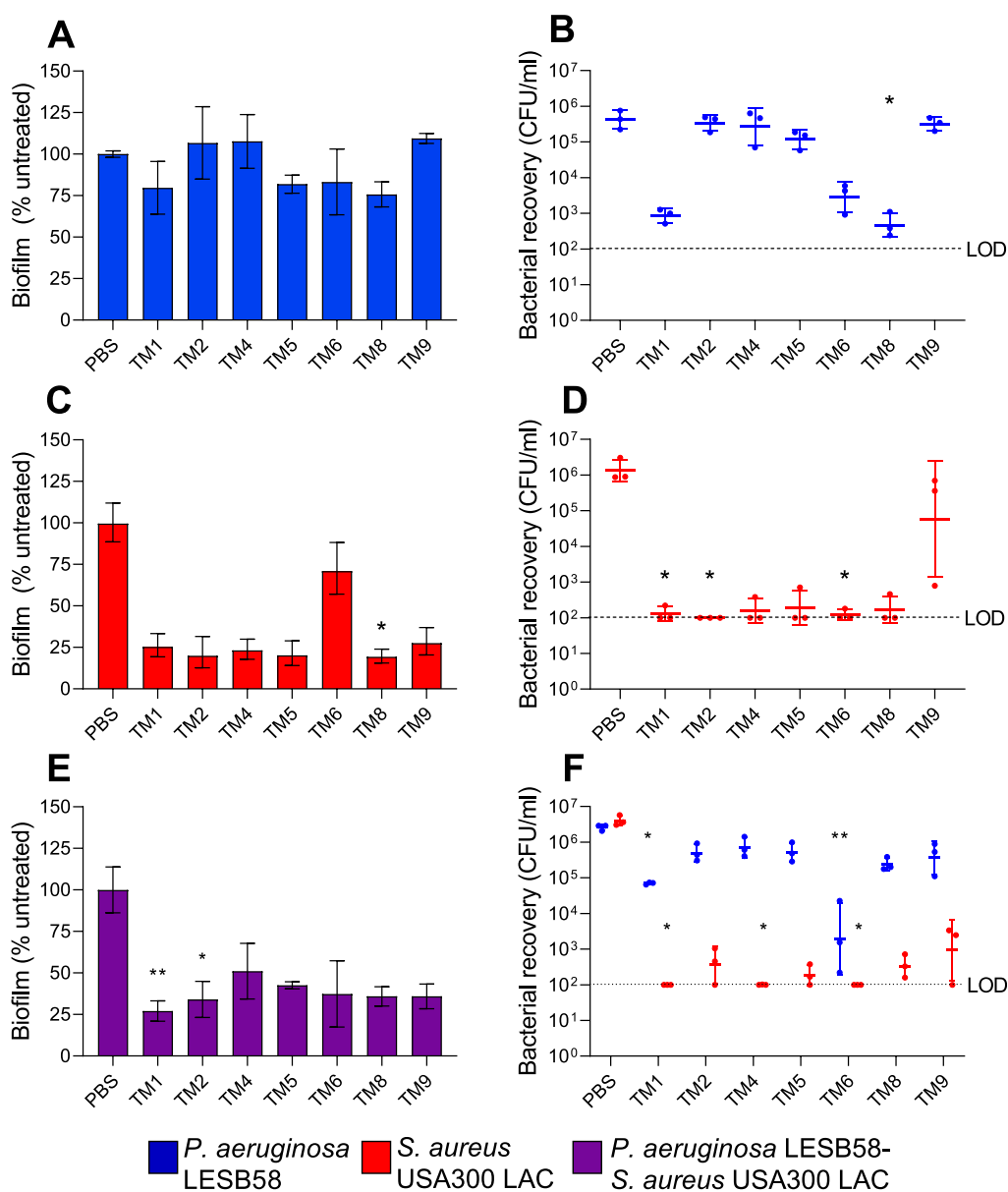


Figure 6. Effect of peptoids on mono- and polymicrobial biofilms. Peptoids (31.25 $\mu\text{g/mL}$) were used to treat biofilms comprising (A,B) *P. aeruginosa* LESB58 (5×10^5 CFU/mL), (C,D) *S. aureus* USA300 LAC (2.5×10^7 CFU/mL), or (E,F) both species. Biofilms were grown for 20–24 h in DMEM-FBS-G prior to treatment and reincubated for another 20–24 h. (A,C,E) Biofilm was quantified by CV staining (%) and (B,D,F) bacterial recovery from biofilms (CFU/mL) determined on selective agar plates. The dotted line indicates the limit of detection (LOD) at 10^2 CFU. Data from three independent experiments each ($n = 3$) are shown as (A,C) mean \pm SEM or geometric mean \pm geometric SD. * $p < 0.05$ and ** $p < 0.01$ according to the Kruskal–Wallis test with Dunn’s correction.

exhibited no apparent cytotoxicity in vitro when applied to the apical surface of three-dimensional tissue models of primary human gingival epithelial cells grown at the air–liquid interface, at concentrations as high as 256 $\mu\text{g/mL}$ (Figure S4). These results are similar to those described for TM4, TM5, and TM9 with oral epithelial cells in a recently published paper.¹⁴

Certain Peptoids Exhibit Antibiofilm Activity against ESKAPE Pathogens. We further investigated the antibiofilm activity of TM peptoids against all ESKAPE pathogens (Figure 4). At 1.56 $\mu\text{g/mL}$, TM1 exhibited slight but significant inhibition of biofilm formation by *S. aureus*, *K. pneumoniae*, *A. baumannii*, *P. aeruginosa*, and *E. cloacae* relative to a PBS control. At 6.25 $\mu\text{g/mL}$, TM1 reduced the biomass of preformed biofilms for *S. aureus*, *K. pneumoniae*, and *P.*

aeruginosa and reduced metabolic activity of all ESKAPE pathogens in the biofilm growth state.

TM2 inhibited biofilm formation by *E. faecium* and *E. cloacae* only but slightly reduced the biomass of preformed biofilms for *K. pneumoniae* and *P. aeruginosa* and attenuated biofilm metabolic activity for all species except *P. aeruginosa*. TM3 and TM4 only exhibited significant biofilm inhibition against *E. cloacae* and showed minor reduction of preformed biofilm biomass for *S. aureus* and/or *P. aeruginosa*. However, these peptoids reduced biofilm metabolic activity for *E. faecium*, *S. aureus*, and *K. pneumoniae*. TM5 inhibited biofilm formation by *K. pneumoniae* and *P. aeruginosa* but reduced biofilm biomass of *S. aureus* and *K. pneumoniae* and reduced biofilm metabolic activity for the same pathogens and for *E. faecium* and *P. aeruginosa*.

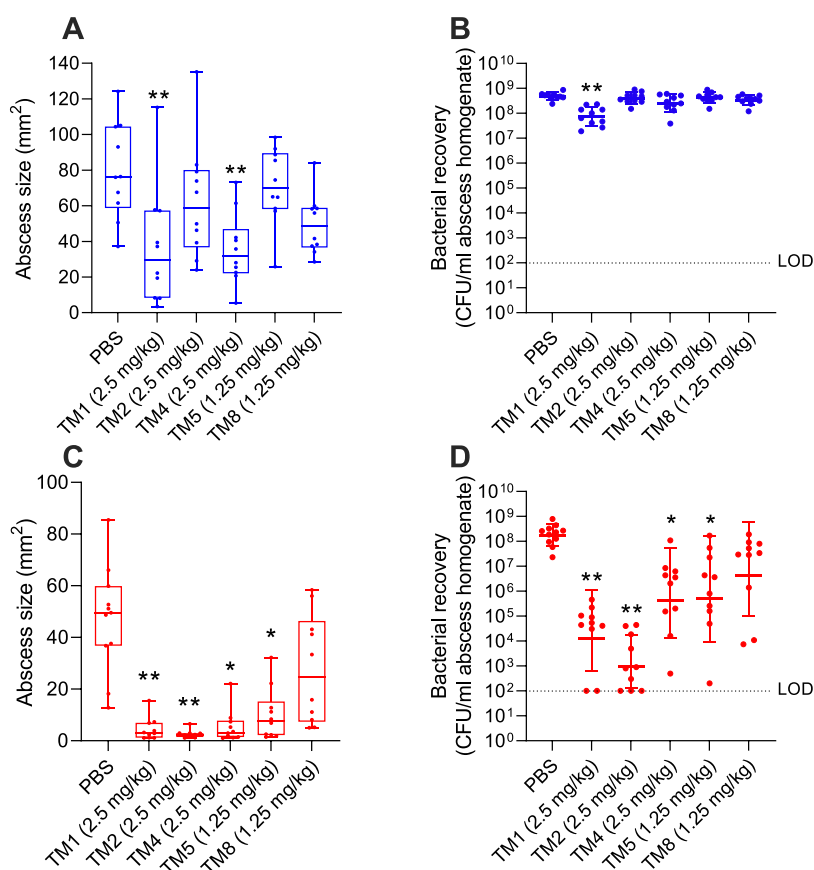


Figure 7. In vivo activity of the maximum tolerated concentration of peptoids against clinical isolates of *P. aeruginosa* (A,B) and *S. aureus* (C,D). Mice were subcutaneously inoculated with $\sim 2.5\text{--}5 \times 10^7$ CFU *P. aeruginosa* LESB58 or $\sim 3\text{--}5.5 \times 10^7$ CFU *S. aureus* USA300 LAC and treated with peptoid or PBS 1 h later. After 3 days, mice were euthanized, abscesses were measured (A,C) and then collected for bacterial enumeration (B,D). Results are displayed as median with whiskers to min and max (A,C) or geometric mean \pm geometric SD (B,D). * $p < 0.05$ and ** $p < 0.01$ different from PBS according to the Kruskal–Wallis test. $n = 10$. LOD is displayed as a dotted line at 10^2 CFU.

TM8, TM9, and TM10 inhibited biofilm formation by all pathogens except *E. faecium* and *A. baumannii*, although the effect of TM9 against *S. aureus* biofilm formation was not significant. The biomass of *S. aureus* and *K. pneumoniae* preformed biofilms was impacted across these peptoids, and metabolic activity was reduced for all pathogens except *P. aeruginosa* as well as, in the case of TM10, *E. faecium*, *A. baumannii*, and *E. cloacae*.

Peptoids Exhibited Superior Antibiofilm Activity against *S. aureus* in Both Mono- and Polymicrobial Biofilms. The host environment is an important factor to consider for the assessment of novel therapeutic treatments. It has become increasingly recognized that the host environment affects drug activity.^{32,33} Therefore, we selected *P. aeruginosa* and *S. aureus* to represent Gram-negative and Gram-positive organisms, respectively, to further assess peptoid activity under host-mimicking conditions. Tissue culture medium supplemented with serum and glucose (DMEM-FBS-G) was used to assess antimicrobial and antibiofilm activity of the peptoids. Overall peptoid antimicrobial activity was enhanced against *S. aureus* under these conditions (Table S1). In order to assess the antibiofilm activity of the peptoids, we performed eradication experiments of monomicrobial *P. aeruginosa* and *S. aureus* and polymicrobial *P. aeruginosa*–*S. aureus* preformed biofilms in DMEM-FBS-G. While none of the peptoids reduced the biomass of *P. aeruginosa* biofilms significantly under these conditions (Figure 5A), all of the peptoids showed

>50% biomass reduction against *S. aureus* at all concentrations tested (Figure 5B). Intriguingly, all of the peptoids achieved a reduction in polymicrobial biofilm mass by $\sim 50\%$, except for TM9 (Figure 5C). We further determined $31.25 \mu\text{g/mL}$ as a potential, effective antibiofilm concentration across all investigated peptoids against both mono- and polymicrobial biofilms (Figure 6). At this concentration, TM1, TM5, TM6, and TM8 reduced 17–25% of *P. aeruginosa* biomass when compared to the PBS-treated control biofilms (Figure 6A). Intriguingly, TM8 reduced *P. aeruginosa* significantly by 1000-fold, and although not significant, TM1 ($p = 0.09$) and TM6 ($p = 0.22$) also visually reduced *P. aeruginosa* bacterial numbers by ~ 1000 -fold and 100-fold, respectively (Figure 6B). Against *S. aureus*, all of the peptoids visually reduced biomass by at least 70% except TM6, which had a 28% reduction. TM8 was the only peptoid that significantly reduced *S. aureus* biomass (by 81%) (Figure 6C). *S. aureus* cells were significantly reduced by at least 10,000-fold in wells treated with TM1, TM2, and TM6 (i.e., CFU recovery below limit of detection) (Figure 6D).

Overall, a >50% reduction of biomass was observed for all peptoids against *P. aeruginosa*–*S. aureus* polymicrobial biofilms (Figure 6E). TM1 and TM2 reduced biomass significantly ($p = 0.003$) by 73% and ($p = 0.04$) by 66%, respectively. Biofilms treated with TM4 showed higher biomass staining but significantly ($p = 0.04$) reduced *S. aureus* within the biofilm below the limit of detection of 10^2 CFU/mL. TM1 and TM6

also reduced *S. aureus* within the biofilm significantly ($p = 0.03$ and $p = 0.002$, respectively) below the limit of detection; however, the majority of peptoids reduced viable *S. aureus* within the biofilm by $\sim 10,000$ -fold, thus indicating that the remaining biofilms were *P. aeruginosa*-dominant. By comparison, the majority of the peptoids reduced *P. aeruginosa* by ~ 10 -fold within the polymicrobial biofilm. TM1 and TM6 were the only peptoids that significantly reduced *P. aeruginosa*, by 100-fold ($p = 0.02$) and 1,000-fold ($p = 0.001$), respectively (Figure 6F).

Peptoids Reduced *S. aureus* Abscess Size and Bacterial Load In Vivo. We formed skin abscesses in mice using *P. aeruginosa* and *S. aureus* as representatives of the Gram-negative and Gram-positive ESKAPE pathogens (Figure 7). One hour post-infection, peptoids were administered at their maximum tolerated dose (2.5 mg/kg for TM1, TM2, and TM4 and 1.25 mg/kg for TM5 and TM8; Table S3) and compared to a PBS control. TM1 reduced *P. aeruginosa* abscess size by a factor of ~ 2 (from 79.6 to 36.8 mm²) and significantly reduced bacterial load ~ 5 -fold (from 4.9×10^8 to 8.2×10^7 CFU/mL). TM4 also reduced abscess sizes ~ 2 -fold to 35.5 mm² but did not significantly impact on bacterial load (3.2×10^8 CFU/mL). Other peptoids did not significantly impact on abscess size or bacterial load in vivo when compared to the PBS control. Intriguingly, more peptoids maintained their activity toward *S. aureus* infection in vivo. TM1 and TM2 showed the greatest reduction in abscess size ($>90\%$, from 47.2 to 4.6 and 2.7 mm², respectively) and also the greatest reduction in bacterial load (by $>10,000$ -fold, from 2.3×10^8 to 4.9×10^4 CFU/mL for TM1, and by $>100,000$ -fold to 8.5×10^2 CFU/mL for TM2). TM4 and TM5 also reduced abscess size by $\sim 80\%$ to 5.6 and 10.2 mm², respectively, and reduced bacterial load by ~ 1000 -fold. TM8 insignificantly reduced *S. aureus* abscess size as well as bacterial burden.

DISCUSSION

Antimicrobial resistance is rapidly accelerating, thus creating an urgent need for new antibacterial drugs. Here, we explored a family of peptoids comprising two well-studied compounds TM1 and TM5 and eight peptoids (TM2–TM4 and TM6–TM10) which are variants and molecular hybrids of TM1 and TM5. We used these peptoids to treat ESKAPE pathogens and investigated their activity against Gram-negative *P. aeruginosa* and Gram-positive *S. aureus* under host-mimicking conditions and in a very-challenging high-density cutaneous mouse abscess infection model. These peptoids varied in chain length (6mer–12mer), net positive charge, and hydrophobicity by the inclusion of varying numbers of Nspe monomers, covalently bound alkyl chains, and halogen substitutions.

The majority of these peptoids exhibited antimicrobial activity against all ESKAPE pathogens, except for the 6-mer TM7, which was found to have no antimicrobial or antibiofilm activity (Table 1, Figure 4). This correlated with TM7 being the only peptoid not found to self-assemble to some degree in solution, which was likely due to its short length. All of the other peptoids investigated by SAXS revealed strong intermolecular interactions promoting self-assembly into larger bundled or micellar structures (Figure 1). The critical micellar concentrations (CMCs) as estimated by modeling of SAXS data generally seem to be below the minimum inhibitory concentration (MIC) range (in the order of 1 $\mu\text{g/mL}$), which supports our hypothesis that sufficient self-assembly contributed to both antimicrobial and antibiofilm activity of

peptoids. Self-assembly into defined multimers has rarely been observed in natural AMPs despite their amphiphilic properties.³⁴ However, one exception is the human cathelicidin LL-37,^{27,35} which formed larger tetrameric helical bundles according to the current study (Figures 2 and 3). In a previous study, TM1, TM6, and LL-37 were all found to cross bacterial membranes, bind to DNA, and also rapidly aggregate bacterial ribosomes in vitro and in vivo, and these phenomena have therefore been suggested as key mechanisms of killing for both cationic, amphipathic peptoids, and peptides.³⁶ We hypothesize that these newly discovered supramolecular peptoid assemblies disassociate when they come in contact with anionic bacterial membranes, explaining the rapid bacterial membrane permeabilization that has been observed for these peptoids (unpublished data, manuscript in preparation).

Other peptoids with intriguing activity are TM3 and TM10; both exhibited antimicrobial activity against *P. aeruginosa* that was comparable to TM1 (the antimicrobial activity of TM3 and TM10 was at least fourfold decreased against other ESKAPE pathogens). TM10 is a lipopeptoid with a similar structure to TM5, TM8, and TM9 (Figures 1 and 3); however, TM10 forms a higher proportion of worm-like micelles (TM5 and TM8 formed only ellipsoidal micelles, while TM9 formed a mixture of 90% ellipsoidal and 10% worm-like micelles, and TM10 60% ellipsoidal and 40% worm-like micelles). We hypothesize that worm-like physical morphology, if too stable, can inhibit antibacterial and antiviral activity, which may therefore account for TM10's reduced activity when compared to its analogues TM5, TM8, and TM9, which exhibited antimicrobial activity within 2–4-fold of TM1. Furthermore, TM10 also recently demonstrated lower antiviral activity when compared to TM9.¹⁴ Given the structural similarity of TM9 and TM10, which differ only in the lengths of their alkyl chains (C10 for TM9 and C13 for TM10), these results suggest that both hydrophobicity and micellar aggregation number contribute to the biological function of peptoids. In line with this, the activity of the YGAAKKAACKAAKAAKAA (AKK) peptides conjugated to fatty acids of varying lengths was lost when the minimal active concentration exceeded the CMC.³⁷ While the conjugation of the AKK peptide with fatty acid tails increased their affinity for anionic lipid membranes, the self-assembled structure (obtained at concentrations above the CMC) apparently could inhibit the efficient binding of the peptide to bacterial cell membranes,³⁷ and we also hypothesize intracellular mechanisms of action, although those were not mentioned in that report. Thus, for alkylated AMPs, optimal activity may require a proper balance between hydrophobicity and self-assembly, which is different for various biological activities (e.g., TM10 showed no antibiofilm activity against *P. aeruginosa*). However, as this hypothesis is based only on results obtained with TM10 together with limited literature references, further studies are warranted that focus more specifically on how morphology and stability of self-assembled structures affects bioactivity, especially in regard to the antibacterial activity of the ellipsoidal micellar versus more extended worm-like structures.

This study suggests that the chemical structure of antimicrobial peptoids is not the only factor that needs to be considered when assessing biological activity: we must also consider their propensity to self-assemble in a physiological aqueous environment. Moreover, various features of the host environment including pH, nutrient availability, and the

presence of albumin also can impact peptoid activity.³⁸ The host environment is known to affect bacterial virulence³⁹ and antibiotic efficacy³³ and can also affect interspecies interactions. Under physiologically relevant conditions, peptoid antimicrobial activity was enhanced against *S. aureus* when compared to results in nutrient-rich laboratory medium (Table S1). Furthermore, the peptoids exhibited potent antibiofilm activity against *S. aureus* in mono- and polymicrobial biofilms but were less active against *P. aeruginosa* (Figures 5 and 6).

The higher antimicrobial and antibiofilm activity of these cationic peptoids toward *S. aureus* compared to *P. aeruginosa* could be attributed at least partially to acidification observed in the *S. aureus*-inoculated wells (Figure S5). It is known that many AMPs, including several that have successfully completed clinical trials,⁴⁰ have pH-dependent activity. This may be caused by protonation of amino acid residues, which can influence their interaction with bacterial membranes⁴¹ and other targets and thereby promote peptide synergy with other membrane-targeting antibiotics and host defense molecules.^{42,43} In an analogous manner, the net positive charge of the presently described cationic peptoids may have increased under the low pH (acidic) conditions observed,^{44,45} thus increasing their affinity for the slightly anionic (lipo)teichoic acids in the cell wall of *S. aureus*.

TM1 and TM6 retained significant activity toward *P. aeruginosa* and *S. aureus* polymicrobial biofilms, whereas other peptoids studied herein were less effective toward at least one of the species compared to their respective activity in monomicrobial infection (Figure 6). TM1 and TM6 are self-assembling peptoids that form a mixture of monomers and mainly dimeric helical bundles. However, they lack halogen substitution and an alkyl tail, both of which are known to increase hydrophobicity and, consequently, the tendency for supramolecular assembly.^{11,13,46} In contrast, peptoids with halogen substituents, such as TM2 (half-substituted with bromination of every other phenyl ring) and TM4 (fully substituted), did not exhibit any antibiofilm activity against *P. aeruginosa* in monomicrobial or polymicrobial biofilms (Figure 6). Previously, it was observed that a library of peptoids similar in structure to the peptoids studied here (and also based on TM1 analogues) were effective against polymicrobial biofilms comprising *Candida albicans*, *E. coli*, and *S. aureus*.⁴⁷ However, as mentioned here, *C. albicans* was less susceptible to the peptoids in polymicrobial biofilms than monomicrobial biofilms. These data highlight the complexity of treating infections based on polymicrobial biofilms and how the interactions between species may impact the effectiveness of treatment strategies using AMPs and peptoids.

The addition of a terminal alkyl tail to peptoids was shown here to enable the supramolecular assembly of core-shell micellar structures, obviously with a significantly higher aggregation number than for the helical bundles formed by TM1 and TM6. Peptoids TM5, TM8, and TM9 all formed ellipsoidal micellar assemblies, with aggregation numbers of approximately 98, 103, and 117 peptoids on average, respectively. These high aggregation numbers are remarkable and suggest that there are intermolecular interactions beyond hydrophobic forces, for example, potential hydrogen bonding between Nlys groups and π - π stacking between Nspe groups. Judging from the aggregation number alone, the physical stability of these ellipsoids would be substantial. This may be beneficial for the effective drugability of these peptoids, since these supramolecular peptoid assemblies seem to act as a sort

of vehicle-free self-controlled delivery system.⁴⁸ This approach is advantageous in the fact that it allows for the elimination of any need for physical encapsulation or for the covalent conjugation of pharmaceutical excipients.⁴⁹ In the subcutaneous abscess infection model presented in this study, mice were injected with peptoids dissolved in PBS without the inclusion of excipients or of delivery vehicles, thus demonstrating this benefit.

Our murine abscess model of infection provides insights into the activity of peptoids in human skin infections. The high densities of bacteria in this model make treatment very challenging, since antibiotics do not work well against high-density infections. Peptoids exhibited significant reduction in bacterial burden under physiologically relevant conditions, when tested against *S. aureus* and little reduction of *P. aeruginosa* reflective of our in vitro antibiofilm data (Figures 5 and 6). The pH of the murine skin abscess remained slightly acidic throughout the course of infection (Figure S6). Although *P. aeruginosa* did not influence the pH of in vitro media when compared to the sterile control (Figure S6), the antibacterial activity of TM1 was reduced (twofold) by adjusting the pH to 5.4–5.9 (Table S2). This might at least partially explain why TM1 reduced the *P. aeruginosa* bacterial load only modestly (~10-fold) in vivo (Figure 7). However, peptoids TM1 and TM4 did substantially reduce the sizes of abscesses formed by *P. aeruginosa* when compared to untreated controls, indicating that the antiabscess activity of peptoids is distinct from their direct antimicrobial activity. This could involve an inhibition of inflammation, as several naturally occurring AMPs have demonstrated previously,⁵⁰ or the inhibition of other host-mediated responses to high-density infections not yet explored. None of TM1, TM2, or TM4 caused toxic side effects at a concentration of 2.5 mg/kg, whereas TM5 and TM8 did. Thus, TM5 and TM8 were administered intraabscess at a lower concentration of 1.25 mg/kg. Since activity of peptoids could be concentration-dependent, comparison of peptoids used at different concentrations was limited.

This constitutes the first report of discrete, limited supramolecular peptoid assemblies with antibacterial activity and further demonstrates that supramolecular assembly has complex effects on bioactivity. This new understanding of how the self-assembly of antimicrobial peptoids can affect both their in vitro and in vivo activity against ESKAPE pathogens can assist us with future molecular design projects. It is notable that many of the best antibacterial peptoids studied here also exhibit antiviral properties, which is also true of the human host defense peptide LL-37 itself. Finally, our results reveal that several of the novel peptoids reported here simultaneously possess antimicrobial, antibiofilm, and antiabscess activity in standard laboratory media and under host-mimicking conditions. Since the selected peptoids studied here retained their activity under diverse, physiologically relevant conditions, they should be considered for further therapeutic development, particularly for treating high-density skin wound infections. We also confirm that these peptoids exhibit no apparent cytotoxicity in vitro with primary human cells at concentrations of up to 256 $\mu\text{g/mL}$, making them exciting drug candidates as a novel class of anti-infectives.

■ MATERIALS AND METHODS

Source of Peptoids and Stock Solutions. The peptoids TM1-10 (see Figure 1) were synthesized manually as

previously described¹⁴ (Supporting Information Subsection 1.1 for details). Peptoids were dissolved in phosphate-buffered saline (PBS), pH = 7.5 (Gibco) and prepared at 2.5 mg/mL stock solutions prior to storage at -80°C .

Small-Angle X-Ray Scattering. Unless noted otherwise, SAXS experiments were performed at ALS beamline 12.3.1 LBNL Berkeley, California, USA,⁵¹ with a detector distance of 2 m and an X-ray wavelength of $\lambda = 1.27 \text{ \AA}$, covering a Q range of 0.009 to 0.4 \AA^{-1} . The data set was calibrated to an absolute intensity scale using water as a primary standard. All experiments were performed at 20°C , and data were processed as previously described.⁵²

TM7 and TM10 were measured using a Bruker NANO-STAR equipped with a microfocus X-ray source ($I\mu\text{S}$ Cu, Incoatec, Germany) and a VANTEC-2000 detector. Raw scattering data were calibrated to the absolute intensity scale using water as a primary standard and radially averaged in order to obtain the 1D scattered intensity profile as a function of the scattering vector, with a wavelength of 1.54 \AA . The modeling fit analysis of the scattering data is explained in detail in Subsection 1.2 of the Supporting Information.

Bacterial Strains and Growth Conditions. Bacterial strains used in this study were *E. faecium* #2–1 (BEI resources, NR31909), *S. aureus* USA300 LAC,⁵³ *K. pneumoniae* KPLN649,⁵⁴ *A. baumannii* AB5075,⁵⁵ *P. aeruginosa* LESB58,⁵⁶ and *E. cloacae* 218R1.⁵⁷ All organisms were streaked onto lysogeny broth (LB) or double yeast tryptone (dYT) agar plates from frozen stocks and grown at 37°C . When needed, overnight liquid subcultures were grown from a single colony with shaking (250 rpm) for no more than 16 h. Bacterial growth was monitored using a spectrophotometer (Eppendorf, Mississauga, ON).

Cytotoxicity Assay. Normal human gingival epithelial cells, obtained from MatTek (EpiGingival), were grown at an air–liquid interface at 37°C . Serial dilutions of peptoids were prepared from stocks, resulting in a final concentration of 64–256 μM . Peptoids (100 μL) were applied to the apical surface of cultures for 3 h. Cell viability was quantified using the CyQUANT MTT Cell Viability Assay (Thermo Fisher), following the manufacturer's instructions. OD_{540} was scanned, and survival relative to untreated cultures (%) was calculated. The experiment was performed in triplicate. Ethanol was used as a positive control.

Biofilm Growth Conditions. *A. baumannii*, *P. aeruginosa*, and *E. cloacae* biofilms were grown in Mueller–Hinton broth (MHB) for 18–24 h. *S. aureus* biofilms were grown in MHB incubated shaking (200 rpm) for 24 h. *K. pneumoniae* and *E. faecium* biofilms were grown in TSB supplemented with 0.1 and 1% glucose, respectively, for 48 h. For host-mimicking conditions, *P. aeruginosa* and *S. aureus* biofilms were grown in Gibco high-glucose Dulbecco's minimal Eagle's medium (DMEM) supplemented with 5% fetal bovine serum (FBS) (USA origin) and 1% glucose (G) (Sigma-Aldrich), referred to as DMEM-FBS-G. Biofilms were formed as previously described⁵⁸ with minor modifications (see Subsection 1.3 in the Supporting Information).

Antimicrobial Activity of Peptoids. Bacterial susceptibility to peptoids was determined across *ESKAPE* pathogens using the broth microdilution assay⁵⁹ in microtiter plates (Falcon, #351172). Details are included in Subsection 1.4 in the Supporting Information.

Antimicrobial Activity of Peptoids under Host-Mimicking Conditions. MIC of peptoids was determined

using an adapted microdilution broth method⁵⁹ in polypropylene 96-well plates (Greiner Bio-One, #655201) using MHB (Oxoid) and DMEM-FBS-G. Details are included in Subsection 1.5 in the Supporting Information. All tests were performed in triplicate following the Clinical and Laboratory Standards Institute guidelines.^{59,60}

Minimal Biofilm Inhibition (MBIC) and Eradication (MBEC) Assays of *ESKAPE* Pathogens. Biofilm formation conditions across species are included in Subsection 1.6 of the Supporting Information. Data from three biological replicates ($n = 3$) are presented as the percentage of the biofilm, relative to the vehicle control (PBS) at the lowest concentration of tested peptoids (6.25–12.5 $\mu\text{g}/\text{mL}$). Biofilm inhibition and eradication were measured by crystal violet (CV) staining and/or 2,3,5-triphenyl tetrazolium chloride (TTC) reduction as previously described.⁶¹

Biofilm Eradication Experiments under Host-Mimicking Conditions. The eradication methodology was adapted from Haney et al.⁶² with minor modifications (see Subsection 1.7 in the Supporting Information). For eradication experiments with 31.25 $\mu\text{g}/\text{mL}$ peptoids, biofilms were scraped with a sterile cotton swab, submerged in 1 mL of MHB, vortexed, and further used for serial dilutions. Dilutions were plated onto LB agar for bacterial enumeration. For polymicrobial cultures, selective agar plates were used: *Pseudomonas* cetrinide agar (Oxoid) to select for *P. aeruginosa* and 7.5% NaCl plates to select for *S. aureus*. Experiments were repeated three times with five technical replicates each.

Ethics Statement. Animal experiments were performed in accordance with the Canadian Council on Animal Care (CCAC) guidelines and were approved by the University of British Columbia Animal Care Committee (protocol A19-0064) and the University of Otago Animal Welfare Office (protocol 19–125). Details are included in Subsection 1.8 of the Supporting Information.

Subcutaneous Abscess Infection. Peptoid susceptibility of *P. aeruginosa* and *S. aureus* was assessed in vivo using a subcutaneous abscess model, as previously described.⁶³ Modifications are described in Subsection 1.8 of the Supporting Information.

For in vivo pH measurements, mice were subcutaneously injected with 50 μL of *P. aeruginosa*, *S. aureus*, or a mixture (1:1) of *P. aeruginosa* and *S. aureus* (corresponding to $1.25\text{--}2.5 \times 10^7$ CFU). One hour post-infection, mice were punctured with an 18G needle and the InLab Nano Combination Electrode was inserted to measure the voltage (mV). This process was repeated daily, and mice were euthanized on day three.

■ ASSOCIATED CONTENT

SI Supporting Information

The Supporting Information is available free of charge at <https://pubs.acs.org/doi/10.1021/acscinfecdis.1c00536>.

Synthesize and purification of peptoids; theoretical modeling of SAXS data; experimental procedure for cytotoxicity assays and more detailed information on biofilm and MIC assays; SAXS data at different peptoid concentrations; cytotoxicity data; data on antimicrobial activity under host-mimicking conditions; in vivo toxicity data; and data on pH of the localized abscess infection as a function of time (PDF)

■ AUTHOR INFORMATION

Corresponding Author

Annelise E. Barron – Department of Bioengineering, School of Medicine, Stanford University, Stanford, California 94305, United States; orcid.org/0000-0002-0735-6873; Email: aebarron@stanford.edu

Authors

Josefine Eilso Nielsen – Department of Bioengineering, School of Medicine, Stanford University, Stanford, California 94305, United States; Department of Chemistry, University of Oslo, Oslo 0315, Norway; orcid.org/0000-0001-9274-5533

Morgan Ashley Alford – Centre for Microbial Diseases and Immunity Research, University of British Columbia, Vancouver, British Columbia V6T 1Z4, Canada; orcid.org/0000-0002-4446-817X

Deborah Bow Yue Yung – Department of Microbiology and Immunology, University of Otago, Dunedin 9054, New Zealand

Natalia Molchanova – The Molecular Foundry, Lawrence Berkeley National Laboratory, Berkeley, California 94720, United States

John A. Fortkort – Department of Bioengineering, School of Medicine, Stanford University, Stanford, California 94305, United States

Jennifer S. Lin – Department of Bioengineering, School of Medicine, Stanford University, Stanford, California 94305, United States; orcid.org/0000-0001-9169-7410

Gill Diamond – Department of Oral Immunology and Infectious Diseases, University of Louisville, School of Dentistry, Louisville, Kentucky 40202, United States

Robert E. W. Hancock – Centre for Microbial Diseases and Immunity Research, University of British Columbia, Vancouver, British Columbia V6T 1Z4, Canada; orcid.org/0000-0001-5989-8503

Håvard Jenssen – Department of Science and Environment, Roskilde University, Roskilde 4000, Denmark; orcid.org/0000-0003-0007-0335

Daniel Pletzer – Centre for Microbial Diseases and Immunity Research, University of British Columbia, Vancouver, British Columbia V6T 1Z4, Canada; Department of Microbiology and Immunology, University of Otago, Dunedin 9054, New Zealand; orcid.org/0000-0001-5750-7505

Reidar Lund – Department of Chemistry, University of Oslo, Oslo 0315, Norway; orcid.org/0000-0001-8017-6396

Complete contact information is available at:

<https://pubs.acs.org/10.1021/acsinfecdis.1c00536>

Author Contributions

[∇]J.E.N., M.A.A., and D.B.Y.Y. contributed equally to the work, and each reserves the right to put their name first on their respective CVs.

Notes

The authors declare the following competing financial interest(s): A.E.B. is a shareholder and member of the Board of Directors of Maxwell Biosciences; G.D., N.M., J.A.F., R.E.W.H. and H.J. are shareholders and consultants for Maxwell Biosciences; D.P. is a consultant for Maxwell Biosciences.

■ ACKNOWLEDGMENTS

J.E.N., H.J., and R.L. gratefully acknowledge NordForsk (project no. 82004) for financial support. J.E.N. also acknowledge financial support from UiO:Life Science and the Norwegian PhD School of Pharmacy. N.M. and H.J. were also funded by the Danish Council for Independent Research, Technology and Production (project no. 4005-00029). A.E.B., J.F., J.S.L., and J.E.N. acknowledge funding from the U.S. Public Health Services (an NIH Pioneer award to Annelise Barron, NIH/NIA grant # 1DP1 OD029517-01). MAA holds a UBC Killam Doctoral Scholarship, Four-Year Fellowship, and CIHR Vanier Graduate Scholarship. We also gratefully acknowledge funding to R.E.W.H. from the Canadian Institutes for Health Research grant FDN-154287 and Michael Smith Foundation for Health Research grant 17774. REWH holds a Canada Research Chair in Health and Genomics and a UBC Killam Professorship. DP acknowledges funding from the University of Otago Research Grant, the Otago Medical Research Foundation Grant (AG388) and Maxwell Biosciences. We also thank Dr. Allan Gamble at the University of Otago for his help with the pH microelectrode experiments. We also thank Erika Figgins at the University of Louisville for support with the in vitro cytotoxicity experiments. Parts of this work were conducted at the Advanced Light Source (ALS), a national user facility operated by Lawrence Berkeley National Laboratory on behalf of the Department of Energy, Office of Basic Energy Sciences, through the Integrated Diffraction Analysis Technologies (IDAT) program, supported by DOE Office of Biological and Environmental Research. Additional support comes from the National Institute of Health project ALS-ENABLE (P30 GM124169) and a High-End Instrumentation grant S10OD018483. We thank Dr. Gregory Hura and Kathryn Burnett at ALS for support during the SAXS experiment. Work at the Molecular Foundry was supported by the Office of Science, Office of Basic Energy Sciences, of the U.S. Department of Energy under contract no. DE-AC02-05CH11231. We gratefully acknowledge Dr. Michael Connolly and Dr. Behzad Rad at the Molecular Foundry for assistance with peptoid synthesis and sample preparation equipment. We acknowledge use of the Norwegian national infrastructure for X-ray diffraction and scattering (RECX).

■ ABBREVIATIONS

A. baumannii, *Acinetobacter baumannii*; AMP, antimicrobial peptide; *C. albicans*, *Candida albicans*; CFU, colony-forming unit; CMC, critical micellar concentration; CV, crystal violet; DMEM, Dulbecco's minimal Eagle's medium; DNA, deoxyribonucleic acid; dYT, double yeast tryptone; *E. Cloacae*, *Enterobacter cloacae*; *E. faecium*, *Enterococcus faecium*; ESKAPE, *Enterococcus faecium*, *Staphylococcus aureus*, *Klebsiella pneumoniae*, *Acinetobacter baumannii*, *Pseudomonas aeruginosa*, and *Enterobacter sp*; FBS, fetal bovine serum; *K. pneumoniae*, *Klebsiella pneumoniae*; LB, lysogeny broth; MHB, Mueller–Hinton Broth; NLys, N-(4-aminobutyl)glycine; Nspe, (S)-N-(1-phenylethyl)amine; *P. aeruginosa*, *Pseudomonas aeruginosa*; PBS, phosphate-buffered saline; *S. aureus*, *Staphylococcus aureus*; SAXS, small-angle X-ray scattering; TTC, 2,3,5-triphenyl tetrazolium chloride

REFERENCES

- (1) Namivandi-Zangeneh, R.; Wong, E. H. H.; Boyer, C. Synthetic Antimicrobial Polymers in Combination Therapy: Tackling Antibiotic Resistance. *ACS Infect. Dis.* **2021**, *7*, 215–253.
- (2) Sinha, R.; Shukla, P. Antimicrobial peptides: recent insights on biotechnological interventions and future perspectives. *Protein Pept. Lett.* **2019**, *26*, 79–87.
- (3) Jenssen, H.; Hamill, P.; Hancock, R. E. W. Peptide antimicrobial agents. *Clin. Microbiol. Rev.* **2006**, *19*, 491–511.
- (4) Pletzer, D.; Mansour, S. C.; Hancock, R. E. W. Synergy between conventional antibiotics and anti-biofilm peptides in a murine, subcutaneous abscess model caused by recalcitrant ESKAPE pathogens. *PLoS Pathog.* **2018**, *14*, No. e1007084.
- (5) Chongsirawatana, N. P.; Patch, J. A.; Czyzewski, A. M.; Dohm, M. T.; Ivankin, A.; Gidalevitz, D.; Zuckermann, R. N.; Barron, A. E. Peptoids that mimic the structure, function, and mechanism of helical antimicrobial peptides. *Proc. Natl. Acad. Sci. U. S. A.* **2008**, *105*, 2794.
- (6) Park, M.; Jardtzyk, T. S.; Barron, A. E. NMEGylation: a novel modification to enhance the bioavailability of therapeutic peptides. *Biopolymers* **2011**, *96*, 688–693.
- (7) Mojsoska, B.; Zuckermann, R. N.; Jenssen, H. Structure-activity relationship study of novel peptoids that mimic the structure of antimicrobial peptides. *Antimicrob. Agents Chemother.* **2015**, *59*, 4112–4120.
- (8) Brandt, W.; Herberg, T.; Wessjohann, L. Systematic conformational investigations of peptoids and peptoid-peptide chimeras. *Biopolymers* **2011**, *96*, 651–668.
- (9) Sanborn, T. J.; Wu, C. W.; Zuckermann, R. N.; Barron, A. E. Extreme stability of helices formed by water-soluble poly-N-substituted glycines (polypeptoids) with α -chiral side chains. *Biopolymers* **2002**, *63*, 12–20.
- (10) Castelletto, V.; Seitsonen, J.; Tewari, K. M.; Hasan, A.; Edkins, R. M.; Ruokolainen, J.; Pandey, L. M.; Hamley, I. W.; Lau, K. H. A. Self-assembly of minimal peptoid sequences. *ACS Macro Lett.* **2020**, *9*, 494–499.
- (11) Lau, K. H. A.; Castelletto, V.; Kendall, T.; Sefcik, J.; Hamley, I. W.; Reza, M.; Ruokolainen, J. Self-assembly of ultra-small micelles from amphiphilic lipopeptoids. *Chem. Commun.* **2017**, *53*, 2178–2181.
- (12) Sternhagen, G. L.; Gupta, S.; Zhang, Y.; John, V.; Schneider, G. J.; Zhang, D. Solution self-assemblies of sequence-defined ionic peptoid block copolymers. *J. Am. Chem. Soc.* **2018**, *140*, 4100–4109.
- (13) Molchanova, N.; Nielsen, J. E.; Sørensen, K. B.; Prabhala, B. K.; Hansen, P. R.; Lund, R.; Barron, A. E.; Jenssen, H. Halogenation as a tool to tune antimicrobial activity of peptoids. *Sci. Rep.* **2020**, *10*, 14805.
- (14) Diamond, G.; Molchanova, N.; Herlan, C.; Fortkort, J. A.; Lin, J. S.; Figgins, E.; Bopp, N.; Ryan, L. K.; Chung, D.; Adcock, R. S.; Sherman, M.; Barron, A. E. Potent antiviral activity against HSV-1 and SARS-CoV-2 by antimicrobial peptoids. *Pharmaceuticals* **2021**, *14*, 304.
- (15) Uchida, M.; McDermott, G.; Wetzler, M.; Le Gros, M. A.; Myllys, M.; Knoechel, C.; Barron, A. E.; Larabell, C. A. Soft X-ray tomography of phenotypic switching and the cellular response to antifungal peptoids in *Candida albicans*. *Proc. Natl. Acad. Sci.* **2009**, *106*, 19375–19380.
- (16) Chongsirawatana, N. P.; Miller, T. M.; Wetzler, M.; Vakulenko, S.; Karlsson, A. J.; Palecek, S. P.; Mobashery, S.; Barron, A. E. Short alkylated peptoid mimics of antimicrobial lipopeptides. *Antimicrob. Agents Chemother.* **2011**, *55*, 417–420.
- (17) Kapoor, R.; Wadman, M. W.; Dohm, M. T.; Czyzewski, A. M.; Sportmann, A. M.; Barron, A. E. Antimicrobial peptoids are effective against *Pseudomonas aeruginosa* biofilms. *Antimicrob. Agents Chemother.* **2011**, *55*, 3054–3057.
- (18) Mulani, M. S.; Kamble, E. E.; Kumkar, S. N.; Tawre, M. S.; Pardesi, K. R. Emerging strategies to combat ESKAPE pathogens in the era of antimicrobial resistance: a review. *Front. Microbiol.* **2019**, *10*, 539.
- (19) Jamal, M.; Ahmad, W.; Andleeb, S.; Jalil, F.; Imran, M.; Nawaz, M. A.; Hussain, T.; Ali, M.; Rafiq, M.; Kamil, M. A. Bacterial biofilm and associated infections. *J. Chin. Med. Assoc.* **2018**, *81*, 7–11.
- (20) Hughes, G.; Webber, M. A. Novel approaches to the treatment of bacterial biofilm infections. *Br. J. Pharmacol.* **2017**, *174*, 2237–2246.
- (21) Sabnis, A.; Ledger, E. V. K.; Pader, V.; Edwards, A. M. Antibiotic interceptors: creating safe spaces for bacteria. *PLoS Pathog.* **2018**, *14*, No. e1006924.
- (22) Rabin, N.; Zheng, Y.; Opoku-Temeng, C.; Du, Y.; Bonsu, E.; Sintim, H. O. Biofilm formation mechanisms and targets for developing antibiofilm agents. *Future Med. Chem.* **2015**, *7*, 493–512.
- (23) Stokes, J. M.; Lopatkin, A. J.; Lobritz, M. A.; Collins, J. J. Bacterial metabolism and antibiotic efficacy. *Cell Metab.* **2019**, *30*, 251–259.
- (24) Centers for Disease Control and Prevention 2019 AR Threats Report. <https://www.cdc.gov/drugresistance/biggest-threats.html> (accessed 26 Aug).
- (25) Orazi, G.; O'Toole, G. A. "It takes a village": mechanisms underlying antimicrobial recalcitrance of polymicrobial biofilms. *J. Bacteriol.* **2019**, *202*, No. e00530-19.
- (26) Wang, C.; Wang, S.; Li, D.; Chen, P.; Han, S.; Zhao, G.; Chen, Y.; Zhao, J.; Xiong, J.; Qiu, J. Human Cathelicidin Inhibits SARS-CoV-2 Infection: Killing Two Birds with One Stone. *ACS Infect. Dis.* **2021**, *7*, 1545.
- (27) Engelberg, Y.; Landau, M. The Human LL-37 (17-29) antimicrobial peptide reveals a functional supramolecular structure. *Nat. Commun.* **2020**, *11*, 3894.
- (28) Patch, J. A.; Barron, A. E. Helical peptoid mimics of magainin-2 amide. *J. Am. Chem. Soc.* **2003**, *125*, 12092–12093.
- (29) Huang, K.; Wu, C. W.; Sanborn, T. J.; Patch, J. A.; Kirshenbaum, K.; Zuckermann, R. N.; Barron, A. E.; Radhakrishnan, I. A threaded loop conformation adopted by a family of peptoid nonamers. *J. Am. Chem. Soc.* **2006**, *128*, 1733–1738.
- (30) Woolfson, D. N. The design of coiled-coil structures and assemblies. *Adv. Protein Chem.* **2005**, *70*, 79–112.
- (31) Czyzewski, A. M.; Jenssen, H.; Fjell, C. D.; Waldbrook, M.; Chongsirawatana, N. P.; Yuen, E.; Hancock, R. E. W.; Barron, A. E. In vivo, in vitro, and in silico characterization of peptoids as antimicrobial agents. *PLoS One* **2016**, *11*, No. e0135961.
- (32) Belanger, C. R.; Huei-Yi Lee, A.; Pletzer, D.; Dhillon, B. K.; Falsafi, R.; Hancock, R. E. W. Identification of novel targets of azithromycin activity against *Pseudomonas aeruginosa* grown in physiologically relevant media. *Proc. Natl. Acad. Sci.* **2020**, *117*, 33519.
- (33) Ersoy, S. C.; Heithoff, D. M.; Barnes, L.; Tripp, G. K.; House, J. K.; Marth, J. D.; Smith, J. W.; Mahan, M. J. Correcting a fundamental flaw in the paradigm for antimicrobial susceptibility testing. *EBioMedicine* **2017**, *20*, 173–181.
- (34) Tian, X.; Sun, F.; Zhou, X.-R.; Luo, S.-Z.; Chen, L. Role of peptide self-assembly in antimicrobial peptides. *J. Pept. Sci.* **2015**, *21*, 530–539.
- (35) Sancho-Vaello, E.; François, P.; Bonetti, E.-J.; Lillie, H.; Finger, S.; Gil-Ortiz, F.; Gil-Carton, D.; Zeth, K. Structural remodeling and oligomerization of human cathelicidin on membranes suggest fibril-like structures as active species. *Sci. Rep.* **2017**, *7*, 15371.
- (36) Chongsirawatana, N. P.; Lin, J. S.; Kapoor, R.; Wetzler, M.; Rea, J. A. C.; Didwania, M. K.; Contag, C. H.; Barron, A. E. Intracellular biomass flocculation as a key mechanism of rapid bacterial killing by cationic, amphipathic antimicrobial peptides and peptoids. *Sci. Rep.* **2017**, *7*, 16718.
- (37) Chu-Kung, A. F.; Nguyen, R.; Bozzelli, K. N.; Tirrell, M. Chain length dependence of antimicrobial peptide-fatty acid conjugate activity. *J. Colloid Interface Sci.* **2010**, *345*, 160–167.
- (38) Sabath, L. D. Six factors that increase the activity of antibiotics in vivo. *Infection* **1978**, *6*, S67–S71.
- (39) Pulkkinen, K.; Pekkala, N.; Ashrafi, R.; Hämäläinen, D. M.; Nkembeng, A. N.; Lipponen, A.; Hiltunen, T.; Valkonen, J. K.; Taskinen, J. Effect of resource availability on evolution of virulence

and competition in an environmentally transmitted pathogen. *FEMS Microbiol. Ecol.* **2018**, *94*, fty060.

(40) Malik, E.; Dennison, S. R.; Harris, F.; Phoenix, D. A. pH dependent antimicrobial peptides and proteins, their mechanisms of action and potential as therapeutic agents. *Pharmaceuticals* **2016**, *9*, 67.

(41) Jimenez, C. J.; Tan, J.; Dowell, K. M.; Gadbois, G. E.; Read, C. A.; Burgess, N.; Cervantes, J. E.; Chan, S.; Janda, A.; Karanik, T.; Lee, J. J.; Ley, M. C.; McGeehan, M.; McMonigal, A.; Palazzo, K. L.; Parker, S. A.; Payman, A.; Soria, M.; Verheyden, L.; Vo, V. T.; Yin, J.; Calkins, A. L.; Fuller, A. A.; Stokes, G. Y. Peptoids advance multidisciplinary research and undergraduate education in parallel: Sequence effects on conformation and lipid interactions. *Biopolymers* **2019**, *110*, No. e23256.

(42) Sawyer, J. G.; Martin, N. L.; Hancock, R. E. Interaction of macrophage cationic proteins with the outer membrane of *Pseudomonas aeruginosa*. *Infect. Immun.* **1988**, *56*, 693–698.

(43) Lehrer, R. I.; Lichtenstein, A. K.; Ganz, T. Defensins: antimicrobial and cytotoxic peptides of mammalian cells. *Annu. Rev. Immunol.* **1993**, *11*, 105–128.

(44) Walkenhorst, W. F.; Klein, J. W.; Vo, P.; Wimley, W. C. pH dependence of microbe sterilization by cationic antimicrobial peptides. *Antimicrob. Agents Chemother.* **2013**, *57*, 3312–3320.

(45) Gan, B. H.; Gaynord, J.; Rowe, S. M.; Deingruber, T.; Spring, D. R. The multifaceted nature of antimicrobial peptides: current synthetic chemistry approaches and future directions. *Chem. Soc. Rev.* **2021**, *50*, 7820.

(46) Gong, H.; Sani, M.-A.; Hu, X.; Fa, K.; Hart, J. W.; Liao, M.; Hollowell, P.; Carter, J.; Clifton, L. A.; Campana, M.; Li, P.; King, S. M.; Webster, J. R. P.; Maestro, A.; Zhu, S.; Separovic, F.; Waigh, T. A.; Xu, H.; McBain, A. J.; Lu, J. R. How do self-assembling antimicrobial lipopeptides kill bacteria? *ACS Appl. Mater. Interfaces* **2020**, *12*, 55675–55687.

(47) Luo, Y.; Bolt, H. L.; Eggmann, G. A.; McAuley, D. F.; McMullan, R.; Curran, T.; Zhou, M.; Jahoda, P. C. A. B.; Cobb, S. L.; Lundy, F. T. Peptoid efficacy against polymicrobial biofilms determined by using propidium monoazide-modified quantitative PCR. *Chembiochem* **2017**, *18*, 111–118.

(48) Yang, M.; Xu, D.; Jiang, L.; Zhang, L.; Dustin, D.; Lund, R.; Liu, L.; Dong, H. Filamentous supramolecular peptide–drug conjugates as highly efficient drug delivery vehicles. *Chem. Commun.* **2014**, *50*, 4827–4830.

(49) Tyrrell, Z. L.; Shen, Y.; Radosz, M. Fabrication of micellar nanoparticles for drug delivery through the self-assembly of block copolymers. *Prog. Polym. Sci.* **2010**, *35*, 1128–1143.

(50) Alford, M. A.; Baquir, B.; Santana, F. L.; Haney, E. F.; Hancock, R. E. W. Cathelicidin host defense peptides and inflammatory signaling: striking a balance. *Front. Microbiol.* **2020**, *11*, 1902.

(51) Classen, S.; Hura, G. L.; Holton, J. M.; Rambo, R. P.; Rodic, I.; McGuire, P. J.; Dyer, K.; Hammel, M.; Meigs, G.; Frankel, K. A.; Tainer, J. A. Implementation and performance of SIBYLS: a dual endstation small-angle X-ray scattering and macromolecular crystallography beamline at the Advanced Light Source. *J. Appl. Crystallogr.* **2013**, *46*, 1–13.

(52) Hura, G. L.; Menon, A. L.; Hammel, M.; Rambo, R. P.; Poole, F. L., II; Tsutakawa, S. E.; Jenney, F. E., Jr.; Classen, S.; Frankel, K. A.; Hopkins, R. C.; Yang, S.-j.; Scott, J. W.; Dillard, B. D.; Adams, M. W. W.; Tainer, J. A. Robust, high-throughput solution structural analyses by small angle X-ray scattering (SAXS). *Nat. Methods* **2009**, *6*, 606–612.

(53) Centers for Disease Control and Prevention. Outbreaks of community-associated methicillin-resistant *Staphylococcus aureus* skin infections—Los Angeles County, California, 2002–2003. *MMWR Morb. Mortal. Wkly. Rep.* **2003**, *52*, 88.

(54) Behroozian, S.; Svensson, S. L.; Davies, J.; Blaser, M. J. Kisameet clay exhibits potent antibacterial activity against the ESKAPE pathogens. *mBio* **2016**, *7*, No. e01842-15.

(55) Jacobs, A. C.; Thompson, M. G.; Black, C. C.; Kessler, J. L.; Clark, L. P.; McQueary, C. N.; Gancz, H. Y.; Corey, B. W.; Moon, J.

K.; Si, Y.; Owen, M. T.; Hallock, J. D.; Kwak, Y. I.; Summers, A.; Li, C. Z.; Rasko, D. A.; Penwell, W. F.; Honnold, C. L.; Wise, M. C.; Waterman, P. E.; Lesho, E. P.; Stewart, R. L.; Actis, L. A.; Palys, T. J.; Craft, D. W.; Zurawski, D. V. AB5075, a highly virulent isolate of *Acinetobacter baumannii*, as a model strain for the evaluation of pathogenesis and antimicrobial treatments. *mBio* **2014**, *5*, No. e01076-14.

(56) Cheng, K.; Smyth, R. L.; Govan, J. R.; Doherty, C.; Winstanley, C.; Denning, N.; Heaf, D. P.; van Saene, H.; Hart, C. A. Spread of beta-lactam-resistant *Pseudomonas aeruginosa* in a cystic fibrosis clinic. *Lancet* **1996**, *348*, 639–642.

(57) Marchou, B.; Bellido, F.; Charnas, R.; Lucain, C.; Pechère, J. C. Contribution of beta-lactamase hydrolysis and outer membrane permeability to ceftriaxone resistance in *Enterobacter cloacae*. *Antimicrob. Agents Chemother.* **1987**, *31*, 1589–1595.

(58) Coffey, B. M.; Anderson, G. G. Biofilm formation in the 96-well microtiter plate. *Pseudomonas Methods and Protocols*; Springer, 2014; pp 631–641.

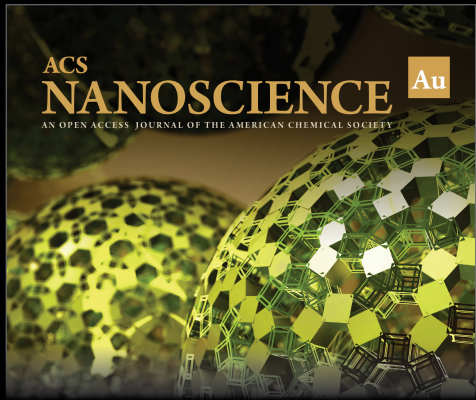
(59) Wiegand, I.; Hilpert, K.; Hancock, R. E. W. Agar and broth dilution methods to determine the minimal inhibitory concentration (MIC) of antimicrobial substances. *Nat. Protoc.* **2008**, *3*, 163–175.

(60) Clinical and Laboratory Standards Institute, *Performance Standards for Dilution Antimicrobial Susceptibility Tests for Bacteria that Grow Aerobically*, 11th ed.; Clinical and Laboratory Standards Institute: Wayne, PA, 2018.

(61) Haney, E. F.; Trimble, M. J.; Hancock, R. E. W. Microtiter plate assays to assess antibiofilm activity against bacteria. *Nat. Protoc.* **2021**, *16*, 2615–2632.

(62) Haney, E.; Trimble, M.; Cheng, J.; Vallé, Q.; Hancock, R. Critical assessment of methods to quantify biofilm growth and evaluate antibiofilm activity of host defence peptides. *Biomolecules* **2018**, *8*, 29.


(63) Pletzer, D.; Mansour, S. C.; Wuerth, K.; Rahanjam, N.; Hancock, R. E. W. New mouse model for chronic infections by Gram-negative bacteria enabling the study of anti-infective efficacy and host-microbe interactions. *mBio* **2017**, *8*, No. e00140-17.




ACS
NANOSCIENCE Au
AN OPEN ACCESS JOURNAL OF THE AMERICAN CHEMICAL SOCIETY

Editor-in-Chief: **Prof. Shelley D. Minteer**, University of Utah, USA

Deputy Editor:
Prof. Raymond E. Schaak
The Pennsylvania State University, USA

Open for Submissions 

pubs.acs.org/nanoau  ACS Publications
Most Trusted. Most Cited. Most Read.